Published in Ground Water 46, issue 1, 61-68, 2007
which should be used for any reference to this work

Solute and Colloid Transport in Karst Conduits under Low- and High-Flow Conditions

by Nadine Göppert[1] and Nico Goldscheider[2]

[1] Department of Applied Geology, University of Karlsruhe, Kaiserstrasse 12, D-76128 Karlsruhe, Germany
[2] Corresponding author: Center of Hydrogeology, University of Neuchâtel, Rue Emile-Argand 11, CH-2009 Neuchâtel, Switzerland; (41) 32 718 2645; fax: (41) 32 718 2604; nico.goldscheider@unine.ch

Abstract

Solute and colloid transport in karst aquifers under low and high flows was investigated by tracer tests using fluorescent dyes (uranine) and microspheres of the size of pathogenic bacteria (1 μm) and *Cryptosporidium* cysts (5 μm), which were injected into a cave stream and sampled at a spring 2.5 km away. The two types of microspheres were analyzed using an epifluorescence microscope or a novel fluorescence particle counter, respectively. Uranine breakthrough curves (BTCs) were regular shaped and recovery approached 100%. Microsphere recoveries ranged between 27% and 75%. During low flow, the 1-μm spheres displayed an irregular BTC preceding the uranine peak. Only a very few 5-μm spheres were recovered. During high flow, the 1-μm-sphere BTC was regular and more similar to the uranine curve. BTCs were modeled analytically with CXTFIT using a conventional advection dispersion model (ADM) and a two-region nonequilibrium model (2RNE). The results show that (1) colloids travel at higher velocities than solutes during low flow; (2) colloids and solutes travel at similar velocities during high flow; (3) higher maximum concentrations occur during high flow; and (4) the 2RNE achieves a better fit, while the ADM is more robust, as it requires less parameters.

Introduction

Karst aquifers are important fresh water resources but highly vulnerable to contamination, which can easily enter the aquifer through thin soils or via swallow holes, and may be rapidly transported in a network of fractures and conduits. Microbial contamination from agriculture and domestic waste water often constitutes the most serious water quality problem (Drew and Hötzl 1999). Karst aquifers often show strong hydraulic and hydrochemical responses to rainfall, which also result in high variability of suspended matter (turbidity) and bacteria levels (Pronk et al. 2006). Suspended matter can be classified into colloids (less than 1 μm) and larger particles. Mahler et al. (2000) found that a large proportion of fecal bacteria in karst ground water are associated with suspended sediments. These findings underscore the importance of event-based monitoring of bacterial water quality and illustrate the necessity to better understand the processes governing particle transport under different hydrologic conditions.

Tracing techniques are powerful tools for this type of investigations. Solute tracers, such as fluorescent dyes, can be used to study ground water flow and the migration of dissolved contaminants; particulate tracers are surrogates for particle-bound chemical contaminants and pathogens. Lanthanide-labeled clay is an effective but relatively rarely used method of tracing sediment transport (Mahler et al. 1998). Specific bacteriophages and bacteria can be used to simulate pathogen transport (Harvey 1997) but require analysis within 24 h and in some cases legal permission. Some bacteria that were often used as tracers are now classified as pathogens, for example, *Serratia marcescens*. Therefore, fluorescent microspheres are increasingly used as particulate tracers. They are available at different diameters and physicochemical properties and can be considered as surrogates for bacteria (~1 μm) and *Cryptosporidium* cysts (3 to 7 μm) (Emelko and Huck 2004). McCarthy and McKay (2004) note that most previous microsphere traces were done in porous media and at a lab to local field scale, while more experiments

would be required in karst aquifers and at larger field scales (~km flow distance). The few published examples include multitracer tests in the karst aquifer of the mineral springs of Stuttgart, Germany, where low numbers of 1-µm spheres were detected 6 km downstream of the injection well (Goldscheider et al. 2003).

In order to obtain further insight into colloidal transport in karst ground water, the Hölloch cave in the Austro-German Alps has been selected as a test site. The primary goals are (1) to compare the transport of colloids/particles and solutes and (2) to assess the impact of different hydrologic conditions on these transport processes. The study also presents the first application of a relatively new analytical modeling approach for the simulation of tracer breakthrough curves (BTCs) to colloids, and the first application of a fluorescence particle counter for the detection of fluorescent microspheres.

Material and Methods

Test Site

The Hölloch cave in the Austro-German Alps (Figure 1) has a surveyed length of 9.6 km and is part of the Hochifen-Gottesacker karst system developed in Cretaceous sedimentary rocks. The karst aquifer is approximately 100 m thick and underlain by marl. Previous tracer tests (16 injection sites) demonstrated that plunging synclines constitute the main flowpaths, while anticlines act as water divides (Goldscheider 2005). The cave is located in the Mahdtal valley, occupying a syncline that plunges toward ESE below the main valley (Schwarzwassertal). An 80-m shaft at 1450 m provides the entrance. Open-channel flow can be observed in the cave stream, but there are also several siphons. Permanent saturation has to be expected in the lowermost, inaccessible part. The system is drained by the perennial Sägebach spring (Sb) at 1035 m, 2.5 km downgradient from the entrance. The measured spring discharge varies between 170 and 2700 L/s, while the flow rate of the cave stream is generally much lower. The previous study also revealed that the spring receives additional inflow from other parts of the karst area: During low flow, 20% of the water originates from the Mahdtal and 80% from the Schwarzwassertal.

Tracer Tests

Two types of fluorescent polystyrene carboxylate microspheres were used as colloidal/particle tracers: Yellow-Green Microspheres 1.00 µm (Fluoresbrite YG, Polysciences Inc., Eppelheim, Germany) and Bright Blue Microspheres 5.00 µm (FluoSpheres BB, Molecular Probes, Karlsruhe, Germany). The fluorescent dye uranine (sodium fluorescein, BASF, CAS 518-47-8) was used as solute tracer.

On February 26, 2005, the first experiment was carried out during stable low-flow conditions. Two hundred grams of uranine and a mixture of 2 mL of YG 1-µm spheres (corresponding to 9.1×10^{10} particles) and 10 mL of BB 5-µm spheres (3.2×10^{9}) were injected into the cave stream below the entrance shaft at two nearby locations. An automatic sampler (ISCO) was installed at the spring. Due to temperatures down to −20°C, it was placed into a purpose-built heated insulated box. Other springs and streams were sampled manually. The samples were split into two fractions: 200-mL brown plastic bottles to analyze for uranine and 5-µm spheres, and 250-mL brown glass bottles for the 1-µm spheres (methods, see subsequently). The spring discharge, measured by salt dilution, was nearly constant at 172 L/s. The discharge of the cave stream was not measured but estimated at 20 L/s.

A second experiment was done on May 25, 2006, during snowmelt and storm rainfall. Since the cave was inaccessible under such conditions, the tracers were injected into the waterfall dropping into the entrance shaft and immediately joining the cave stream. Only uranine

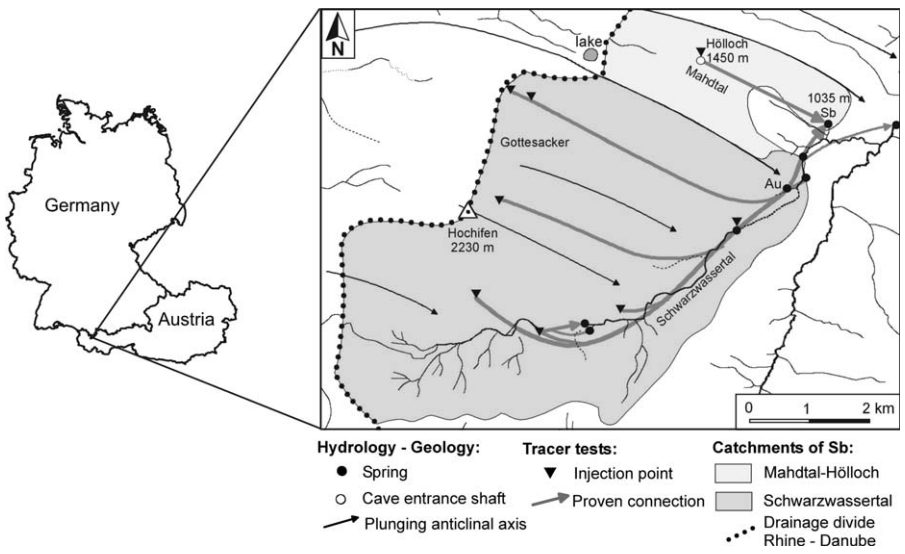

Figure 1. Hydrogeological sketch of the study area (after Goldscheider 2005). Only the new tracer tests between the Hölloch cave and the Sägebach karst spring (Sb) are discussed here. The hydrograph of the Aubach spring (Au) was used to interpolate between the measured discharge values at Sb.

and 1-μm spheres were used for this experiment, in the same quantities as previously. Because of the higher flow rates, shorter sampling intervals were employed. During the experiment, the discharge of the Sägebach spring was measured three times using the salt-dilution method (582, 2691, and 1035 L/s). The hydrograph of the nearby Aubach spring, where discharge is recorded continuously using a pressure probe (data: Landeswasserbauamt Bregenz), was used to interpolate between the measured discharge values of the Sägebach spring. The catchments of both springs overlap (Figure 1), and they show similar responses to rainfall.

Analytical Methods

Uranine was analyzed with a Perkin Elmer LS55 spectrofluorometer. One-micrometer spheres were quantified using a standard method (Käss 1998): homogenization with a sonicator (Sonopuls HD 2200, Bandelin, Berlin, Germany); filtration using 0.8-μm-cellulose nitrate membrane filters (Type 113, Sartorius, Göttingen, Germany) with imprinted reticule; and enumeration using an epifluorescence microscope (Standard FL, Zeiss, Jena, Germany) at an excitation wavelength of 450 to 490 nm and a beam splitter at 510 nm.

Five-micrometer BB spheres were quantified with a novel fluorescence particle counter, that is, a particle counter (Syringe, Markus Klotz GmbH, Bad Liebenzell, Germany) coupled with a fluorescence detector. A 10-mL syringe is used to pass the sample through a 0.2-mm tube illuminated by a laser beam (655 nm). A light detector measures the extinction caused by individual particles, which makes it possible to count particles and measure their equivalent diameters. A detector perpendicular to the laser beam measures light at 670 to 750 nm. The excitation/emission peak wavelengths of the BB spheres are 645/680 nm, respectively. Natural particles do not fluoresce at these wavelengths, so that the tracer spheres can be counted unambiguously. Previous tests in the laboratory revealed that the instrument never erroneously detected BB spheres, even in turbid water samples. The detection limit is one sphere per measured volume. Due to the low injection quantity and the high dilution, low concentration levels were expected and the sampling volume was increased to 100 mL, that is, 10 analyses of each 10 mL.

Evaluation and Modeling Approach

Basic parameters were directly obtained from the BTCs: peak concentration (C_p), first detection time (t_1), peak time (t_p), and the corresponding maximum (v_{max}) and peak (v_p) velocities. Recoveries (R) were calculated from the variable discharge (Q) and concentration (c) data, and injected tracer quantities (M).

$$R = \frac{1}{M} \int_{t=0}^{\infty} (Qc)\mathrm{d}t \qquad (1)$$

The BTCs were further evaluated by fitting two one-dimensional (1D) analytical models to the observed data, an advection dispersion model (ADM), and a two-region nonequilibrium model (2RNE). Both were initially developed for porous media but have also been applied to karst. In conduits, dispersion is most important in flow direction, so that 1D models represent a legitimate simplification. The ADM requires two fit parameters: advection and dispersion; the tracer mass sometimes needs to be fitted too. Advection can be expressed as mean transit time t_0 or mean flow velocity $v = L/t_0$, with L = flowpath length. Dispersion can be expressed as longitudinal dispersion coefficient D, longitudinal dispersivity $\alpha = D/v$ or dispersion parameter $P_D = D/vL$ (reciprocal of the Peclet number). The ADM for a conventional tracer BTC monitored at a fixed site is given as (Kreft and Zuber 1978):

$$c(t) = \frac{M}{Qt_0\sqrt{4\pi p_D \left(\frac{t}{t_0}\right)^3}} \exp\left(-\frac{\left(1-\frac{t}{t_0}\right)^2}{4\,P_D\frac{t}{t_0}}\right) \qquad (2)$$

P_D and t_0 (and sometimes M) are used as fit parameters. Their determination allows v, D, and α to be calculated if a relevant distance L is available. The most straightforward approach is to use linear distances between injection and sampling sites. Real flowpath lengths are always greater but unknown.

The conventional ADM is often not capable of reproducing the tail of BTCs from tracer tests in karst aquifers. Tailing effects in porous media can be explained by exchange between mobile water in large pores and an immobile fluid phase (fine pores and adsorbed water), and described mathematically by a 2RNE (Toride et al. 1993). Field and Pinsky (2000) applied this model for the simulation of BTCs from karst aquifers, where active conduits represent the mobile fluid phase. Several applications revealed that this model is capable of simulating BTCs from tracer tests in karst conduits better than other analytical models (Birk et al. 2005; Geyer et al. 2007).

As the solute tracer used for this study (uranine) is known to behave conservatively in karst aquifers (Käss 1998), solely the following fit parameters were used for the 2RNE: mean flow velocity v, longitudinal dispersion coefficient D, partition coefficient for mobile and immobile fluid regions β ($0 < \beta < 1$; high values indicate a high proportion of mobile water), and mass transfer coefficient ω, describing the exchange rate between the fluid regions ($\omega > 0$; high values indicate high mass transfer). These values were used to calculate the longitudinal dispersion coefficient for the mobile fluid phase $D_m = D/\beta$ and the average mobile fluid velocity $v_m = v/\beta$ (formulas valid for retardation factor = 1, i.e., no retardation).

Strictly spoken, the two models can only be applied to dissolved tracers, while colloids are additionally influenced by filtration, sedimentation, and exclusion (Sirivithayapakorn and Keller 2003). While these processes are comparatively well understood for porous media, there is no satisfactory implementation for karst. Therefore, the models were also used for the microspheres, although the obtained results must be considered with care. CXTFIT (Toride et al. 1999) was used to fit the analytical models to the data. The deterministic equilibrium model in this code is identical to the conventional ADM if retardation and degradation are not considered. The tracer quantities were assumed to be unknown and

fitted to the data. For a better comparison of the results and to avoid artifacts in interpretation (Zhang et al. 2001), BTCs are presented in a normalized form (m^{-3}); that is, all concentrations were divided by the corresponding injection quantities (mass or number of particles).

Results

Tracer Test during Stable Low-flow Conditions

Uranine was first detected at the spring 66.4 h after injection and reached a maximum of 9.25 µg/L after 98.3 h. The BTC has a regular shape, a single maximum, and a short tail (Figure 2). The recovery of 98.5% confirms that the spring is the only relevant outlet of the cave stream. As this experiment was done under well-controlled conditions (constant discharge, direct injection into flowing water, conservative tracer), the BTC was used to test the applicability of the two modeling approaches. Both allow the main part of the BTC to be simulated well, but only the 2RNE simulates perfectly the entire BTC, including the tail, demonstrated by lower residuals and a higher coefficient of determination (Table 1).

The 1-µm spheres display a highly irregular BTC (Figure 3a). Several samples taken after 27 to 57 h contained variable concentrations of microspheres, but concentrations went down to zero again until a continuous curve started after 65 h. The early detections might be explained by alternative pathways in the aquifer, such as fractures with higher flow velocities but low-flow rates between the microspheres injection point and the spring. The main, continuous part of the BTC (after 65 h) matches fairly well with the uranine BTC so that it appears justified to compare this part of the curve with the uranine BTC.

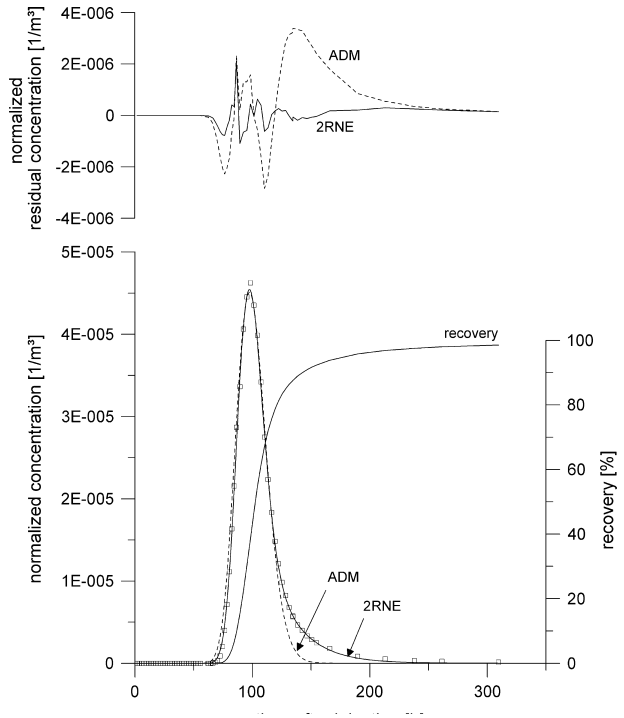

Figure 2. Results for uranine during low flow: observed values (squares), fitted models (ADM and 2RNE), residual concentrations. Constant spring discharge during the experiment: 172 L/s.

The irregularity of the microspheres BTC hampers modeling. To obtain at least a semiquantitative interpretation and to test the applicability of the models to irregular data, the two analytical solutions were fitted to the observed main part of the BTC (i.e., after 65 h), which resulted in very low values of R^2. Therefore, the data point with the greatest residual concentration was removed and a new model run was performed. This procedure was repeated until the criterion $R^2 > 0.8$ was fulfilled, which required removal of four data points (not shown in Figure 3a, since they would exceed the range of the *y*-axis). During the different model runs, *v* and *D* obtained from the ADM did not change significantly, while the fit parameters of the 2RNE varied greatly. This means that the ADM is more robust in this case, while the irregularity of the data prohibits the use of the more sophisticated 2RNE. Therefore, only the results of the ADM are presented and discussed here. The recovery obtained with the corrected data is approximately 75%.

The first 5-µm sphere was detected after 73 h. Subsequent samples contained one to six spheres per 100 mL; the highest value (38/100 mL) occurred after 105 h (Figure 3b). The results prove that particles in the size of *Cryptosporidium* cysts are transported over a distance of 2.5 km, and illustrate the ability of the fluorescence particle counter to detect the tracer spheres at extremely low levels. Due to the concentrations near the detection limit and the irregularity of the BTC, modeling was not considered sensible and the determination of the recovery remains ambiguous. The calculated recovery is 27% when the previously mentioned highest single value is removed and 48% if included.

Tracer Test during Variable High-flow Conditions

Uranine was first detected after 12.8 h. The maximum of 15.6 µg/L occurred after 17.3 h. The 1-µm spheres appeared after 11.5 h and reached a peak concentration of 6120/L after 17.5 h. The BTCs of solute and colloidal tracers display similar transit times, although the microsphere curve is narrower (Figure 4). The recovery is 99.8% for uranine and 42.1% for microspheres, suggesting that colloid attenuation also operates to some degree during high flow. The uranine BTC shows a secondary peak after 30 h. Multipeak BTCs are often explained by multiple pathways (Maloszewski et al. 1992). In the present case, rainfall and variable flow rates are a more likely explanation. There are two possible causes for this second peak: (1) the minimum between the two peaks is due to dilution and (2) the second peak is due to remobilization of uranine by higher flow rates. As the local uranine minimum coincides with the local discharge maximum (Figure 4), the first possibility appears more likely. The BTCs were simulated using the ADM and 2RNE. The 2RNE achieved better fits, mainly of the tails, demonstrated by higher values of R^2. Only the 2RNE curves are shown in Figure 4; Table 1 includes all results.

Table 1
Summary of the Tracer Test Results

				Low Water (2005)		High Water (2006)	
	Property	**Symbol**	**Unit**	**Uranine**	**1-µm Spheres[2]**	**Uranine**	**1-µm Spheres**
Basic data	Injection quantity	M	g, n[1]	200	9.10×10^{10}	200	9.10×10^{10}
	Spring discharge rates	Q	L/s	Constant: 172		Variable: 580–2691	
	Time of first detection	t_1	h	66.4	65.4	12.8	11.5
	Peak time	t_p	h	98.3	83.4	17.3	17.5
	Peak concentration	C_p	µg/L, n/L[1]	9.25	4400	15.63	6120
	Normalized peak concentration	C_p/M	m^{-3}	4.62×10^{-5}	4.84×10^{-5}	7.82×10^{-5}	6.73×10^{-5}
	Maximum velocity	v_{max}	m/h	37.7	38.3	196.1	217.4
	Peak velocity	v_p	m/h	25.4	30.0	144.9	142.9
	Recovery	R	%	98.5	75.1	99.8	42.1
ADM	Mean flow velocity	v	m/h	24.8	28.1	136.9	139.8
	Mean transit time	t_0	h	100.9	89.0	18.3	17.9
	Longitudinal dispersion	D	m^2/h	514	619	2584	224
	Longitudinal dispersivity	α	m	20.8	22.0	18.9	1.60
	Coefficient of determination	R^2	—	0.988	0.814	0.987	0.862
2RNE	Average mobile fluid velocity	v_m	m/h	25.5	n.d.	138.3	146.3
	Corresponding transit time	t_m	h	98.0	n.d.	18.1	17.1
	Longitudinal dispersion, mobile fluid phase	D_m	m^2/h	395.1	n.d.	2239.0	137.5
	Longitudinal dispersivity	α	m	15.5	n.d.	16.2	0.94
	Partition coefficient	β	—	0.92	n.d.	0.93	0.92
	Mass transfer coefficient	ω	—	0.39	n.d.	0.19	1.13
	Coefficient of determination	R^2	—	0.999	n.d.	0.997	0.985

Note: n.d. = not determined (2RNE model not applicable).
[1]Units for uranine, microspheres.
[2]On the basis of the corrected data series.

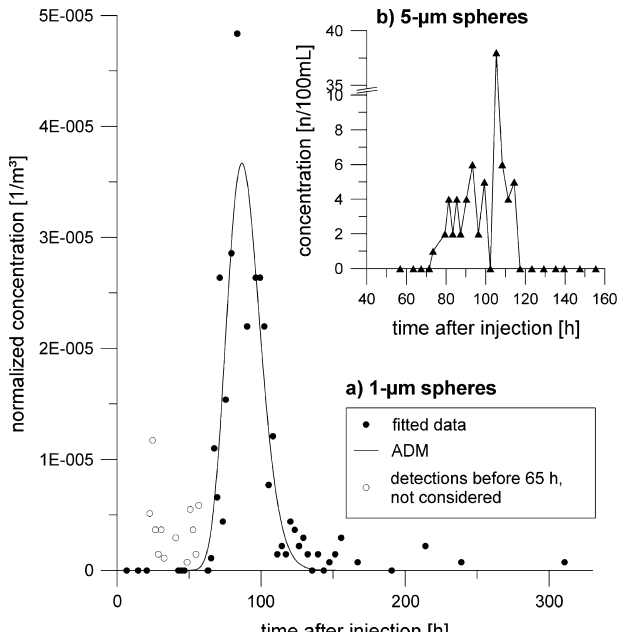

Figure 3. Microspheres during stable low flow, $Q = 172$ L/s: (a) the irregularity of the 1-µm spheres BTC required removal of all positive detections before 65 h (open circles) prior to fitting the 2RNE to the remaining data (closed circles); (b) the steplike pattern of the 5-µm spheres reflects the discrete nature of particle concentrations at extremely low levels.

Discussion

Comparison of the Transport Parameters and Processes

Two limitations have to be considered while comparing the tracer results: the irregularity of the microsphere BTCs in 2005, which hampers modeling, and the effect of the sampling intervals on the precision of the determination of transit times for both tracers.

During low flow, the transit times of the microspheres are shorter than those of uranine; that is, colloids appear to travel at higher velocities (Table 1). The first detection of the microspheres occurred before uranine (even when detections before 65 h are ignored); their peak concentration occurred 15 h earlier; and the ADM gives a mean transit time that is 12 h (12%) shorter. During high flow, the transit times of all tracers are much shorter but very similar for colloids and solutes; for example, the mean transit time for microspheres determined by the ADM is only 0.4 h (2%) shorter than for uranine.

The uranine recovery approached 100% during both experiment, confirming that the Sägebach spring is the only outlet of the system and that uranine behaves conservatively. The recoveries for microspheres were lower, suggesting that some degree of colloid attenuation also occurs in karst conduits. Attenuation processes may include attachment to rock surfaces, filtration in cave

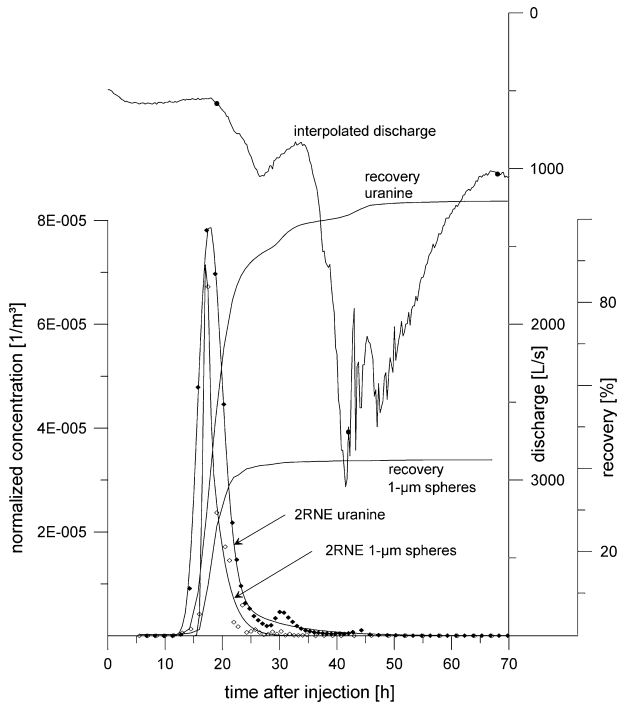

Figure 4. Results during high flow: observed concentrations of uranine (black diamonds) and 1-µm spheres (open diamonds), and simulated BTCs. The hydrograph of the nearby Aubach spring was used to interpolate between the discharge values (black circles) measured at the Sägebach spring.

sediments, and, mainly for the 5-µm spheres, gravitational sedimentation. More microspheres were recovered during low flow (~75%) than during high flow (41%), although one would expect more effective transport during high flow. However, violent flow could also provoke more intense collisions with rock surfaces, and thus more attachment. Additional experiments are required to confirm or infirm this hypothesis.

Dispersive transport can best be discussed by means of the dispersivity α, which eliminates the influence of flow velocity ($\alpha = D/v$) and indicates the variance of velocities, reflected in the width of the BTC. Both models deliver similar dispersivities. For reasons of simplification, only the ADM results are discussed. During low flow, microspheres show slightly higher dispersivity (22 m) than uranine (21 m). During high flow, however, the dispersivity of the microspheres is drastically lower (1.6 m) than the one of uranine (19 m), manifested in a very narrow microsphere BTC. This finding, together with the lower recovery, suggests that the microspheres are effectively transported along the main flow channel but have the tendency to attach to rock surfaces due to intense collisions during high flow.

The partition coefficients β and mass transfer coefficients ω must be interpreted with caution. As the 2RNE did not deliver reliable results for the irregular microsphere BTC during low flow (2005), β and ω values are available only for three BTCs. The partition coefficients obtained from these BTCs are nearly identical (0.92 to 0.93), suggesting a constantly high volume fraction of the mobile fluid region. The mass transfer coefficient for uranine decreases from 0.39 to 0.19 with increasing discharge, indicating less intense mass transfer between mobile and immobile fluid regions during higher flow rates. The mass transfer coefficient for microspheres during high flow (1.13) is substantially higher than for uranine, which can be interpreted as more intense mass transfer for colloids than for solutes.

However, because of the four fit parameters, the 2RNE model tends to create nonunique results. In the present case, nonuniqueness mainly affects the dispersivity and mass transfer coefficient of the high-flow microspheres data: the BTC can be reproduced by different combinations of α and ω, such as very high ω (1.6) and very low α (0.76), as well as lower ω (0.5) and higher α (2.16 m), whereby R^2 remains nearly constantly high at more than 0.97.

Faster transport but lower recovery of colloids with respect to solutes has often been observed in porous media and is explained by exclusion processes; that is, colloids are transported in larger pores (pore exclusion) and in pore centers (size exclusion) where flow velocities are higher, while solutes sample the entire pore volume (Bradford et al. 2004; Keller et al. 2004; Sirivithayapakorn and Keller 2003). At the same time, different filtration processes remove a part of the particles, which explains the lower recovery (McDowellboyer et al. 1986). Toran and Palumbo (1992) examined the effects of fractures on colloidal transport by inserting small tubes into a sand column and found that microspheres traveled at higher velocities than solutes, as they were preferentially transported in the tubes but largely retained in the sand. The tubes also created multiple flowpaths, causing irregular microsphere BTCs.

Studies comparing colloid and solute transport in karst are scarce but consistent with our findings. Auckenthaler et al. (2002) observed that microspheres arrived much faster and at lower recoveries than other tracers, although the BTC is not documented in their paper. Monitoring of natural parameters at karst springs also confirms that colloids and particles (bacteria, turbidity) often precede solutes (organic carbon, nitrate) (Pronk et al. 2006). Mahler et al. (1998) observed that the time of arrival and peak concentrations of lanthanide-labeled clay preceded that of a conservative tracer during normal flow conditions, while the particle tracer was not recovered during low flow, which was explained by sedimentation. A recent study by Harvey et al. (submitted) also reports significantly shorter transit times for microspheres than for a conservative tracer in a karst aquifer.

To date, there is no consistent theory explaining colloid vs. solute transport in karst. Based on our findings and the studies cited previously, the following hypotheses can be formulated:

- Colloids are preferentially transported along the fastest flow lines; solutes sample the entire fluid volume. This exclusion process is most efficient during low flow, as turbulences during high flow cause more homogenous velocity profiles over the conduits' cross-sectional areas. The absolute and relative transit-time differences between colloids and solutes are thus greater during low flow.

- Colloids can be attenuated by attachment to surfaces. Increasing turbulences boost the number and intensity of collisions of colloids with rock surfaces, enabling more attachment. This would explain the lower microsphere recovery observed during high flow. However, higher flow rates also cause higher shear stresses at water–rock interfaces, favoring remobilization of particles. Attachment and detachment processes also depend on the physicochemical properties of the water and colloids.
- Colloids can be lost by sedimentation in low-velocity fluid regions. This process mainly affects larger and denser particles and can cause lower recoveries (or even complete loss during low flow, as observed by Mahler et al. 1998). This type of velocity-related loss function mainly affects particles in slower motion and will thus lead to a statistical increase in flow velocities, and BTCs with less tail.
- If cave sediments are involved, filtration processes come into play, as in porous media.

Influence of Flow Rate and Flow Velocity on Maximum Concentrations

Higher flow rates have two opposing influences on maximum concentrations of tracers or contaminants: On one hand, higher flow rates (Q) mean higher dilution; on the other hand, they cause higher flow velocities (v) and thus narrower BTCs. Transformation of Equation 2 reveals that peak concentration c_p is proportional to v/Q if all other parameters are constant (including tracer recovery). Therefore, the variation of the peak concentrations can be described as:

$$\frac{c_{p,h}}{c_{p,l}} = \frac{\left(\frac{v}{Q}\right)_h}{\left(\frac{v}{Q}\right)_l} \quad (3)$$

where the indexes h and l stand for high- and low-flow conditions.

In the present case, the discharge was constantly 172 L/s during low flow but highly variable during high flow. However, during the period from the tracer injection to the observed uranine peak, discharge was relatively constant at 582 L/s (Figure 4). The corresponding peak velocities are 145 m/h and 25.4 m/h, respectively. Thus, v/Q is 0.249 during high flow and 0.148 during low flow. According to Equation 3, maximum concentrations should thus be 1.7 times higher during high flow than during low flow. The observed maximum concentration of uranine was 15.63 µg/L during high flow and 9.25 µg/L during low flow, that is, 1.7 times higher during high flow. In this case, the simple Equation 3 thus predicts perfectly the influence of flow velocity and flow rate on the maximum concentration.

It is noteworthy that the discharge of the Sägebach spring increased by only a factor of 3.4 during the high-flow tracer test, while flow velocities between the cave and the spring increased by 5.7. In a karst system that includes vadose conduit flow, the opposite would be expected because higher flow rates cause both higher velocities and higher flow-through cross-sectional areas (A). According to the condition of flow continuity ($Q = vA$), discharge should thus increase more than velocity. Deviation from this behavior can be explained by the hydrogeological position of the spring: as shown in Figure 1, the spring is the only drainage point of the Hölloch catchment but receives an additional base flow component from the Schwarzwassertal catchment; both components mix near the spring (Goldscheider 2005). The discharge variations of the cave stream observed by speleologists are much higher than the variations of flow velocities determined by the tracer tests (i.e., the continuity condition is valid, of course). However, the inflow of a large but less variable amount of water near the spring makes the variations of spring discharge smaller than those of flow velocity.

Comparison and Limitations of the Modeling Approaches

Three of the BTCs were reproduced well by both models, while the irregular colloid data from 2005 hamper modeling. Both models allow simulation of the main part of the BTCs, but only the 2RNE allows a near-perfect fit of the tails. The coefficients of determination (R^2) were higher for the 2RNE than for the ADM (Table 1), confirming findings by Field and Pinsky (2000) and Birk et al. (2005). However, the ADM requires only two fit parameters, while four fit parameters were used for the 2RNE, which can cause nonuniqueness; that is, different parameter combinations can simulate the observed data. In the present case, nonuniqueness mainly affects the determination of the mass transfer coefficient and dispersivity of the microspheres BTC from 2006. The ADM is more robust and the obtained results can more easily be interpreted. Therefore, Birk et al. (2005) concluded that the conventional ADM should be considered as a standard technique unless there is good reason to apply more complex approaches.

Apart from mass transfer processes, imperfect experimental conditions can also produce a tail. For example, if the tracer is injected into a borehole, a portion of it may be stored in the cased portion and be slowly released over a prolonged period of time, causing a tail that has nothing to do with transport processes inside the aquifer (Brouyère et al. 2005). Injections via the unsaturated zone, dead water volumes at tapped springs, and uncertainties concerning the natural analytical background can also create pseudotailings. Therefore, the 2RNE can be applied only for the evaluation of tracer tests that were conducted under good experimental conditions.

Conclusions

The tracer results demonstrate that colloids/particles of the same size as pathogenic bacteria (1 µm) and *Cryptosporidium* cysts (5 µm) are transported in this karst conduit system over a 2.5-km distance. The 5-µm spheres were injected only during low flow, in a relatively low quantity, and arrived at the spring at low concentration levels—yet sufficiently high to cause illness if it were infectious cysts. The 1-µm spheres were used during both low and high flow and were effectively transported. Attenuation processes removed a part of the colloids, but their normalized maximum concentrations were similar than those for solutes. During low flow, colloids were found to travel

at higher velocities than solutes. During high flow, all velocities increase, but colloids and solutes show similar velocities.

These findings underscore the vulnerability of karst aquifers to contamination and the need of adequate protection strategies (Panno 2006; Renken et al. 2005). Karst spring monitoring often reveals high levels of fecal bacteria after storm rainfall, but good water quality during low-flow periods. This observation mainly reflects the fact that fecal bacteria often originate from agricultural activities at the land surface. During rainfall events, they are flushed into the aquifer and typically arrive at the springs together with organic carbon and secondary turbidity (a primary turbidity peak may occur due to remobilization of sediments in the conduits) (Pronk et al. 2006). However, the present study demonstrated that particle transport, and thus pathogen transport, can also occur during low flow. Therefore, waste water releases into karst aquifers are generally problematic, even at great distances to a drinking water source.

Acknowledgments

BWPLUS (BWR 23008), the Swiss National Science Foundation (200020-105427), and the Raiffeisen Foundation funded this work. We thank Markus Klotz for the cooperation concerning the particle counter, the speleo group for the injections, Tiburt Fritz and Karl Kessler for various help, and Malcolm Field, Steffen Birk, Chris Smart, and an anonymous reviewer for helpful comments.

References

Auckenthaler, A., G. Raso, and P. Huggenberger. 2002. Particle transport in a karst aquifer: Natural and artificial tracer experiments with bacteria, bacteriophages and microspheres. *Water Science and Technology* 46, no. 1: 131–138.

Birk, S., T. Geyer, R. Liedl, and M. Sauter. 2005. Process-based interpretation of tracer tests in carbonate aquifers. *Ground Water* 43, no. 3: 381–388.

Bradford, S.A., M. Bettahar, J. Simunek, and M.T. van Genuchten. 2004. Straining and attachment of colloids in physically heterogeneous porous media. *Vadose Zone Journal* 3, no. 2: 384–394.

Brouyère, S., G. Carabin, and A. Dassargues. 2005. Influence of injection conditions on field tracer experiments. *Ground Water* 43, no. 3: 389–400.

Drew, D., and H. Hötzl. 1999. *Karst Hydrogeology and Human Activities. Impacts, Consequences and Implications*. Rotterdam, Brookfield: Balkema.

Emelko, M.B., and P.M. Huck. 2004. Microspheres as surrogates for *Cryptosporidium* filtration. *Journal American Water Works Association* 96, no. 3: 94–105.

Field, M.S., and P.F. Pinsky. 2000. A two-region nonequilibrium model for solute transport in solution conduits in karstic aquifers. *Journal of Contaminant Hydrology* 44, no. 3–4: 329–351.

Geyer, T., S. Birk, T. Licha, R. Liedl, and M. Sauter. 2007. Multi-tracer test approach to characterize reactive transport in karst aquifers. *Ground Water* 45, no. 1: 36–45.

Goldscheider, N. 2005. Fold structure and underground drainage pattern in the alpine karst system Hochifen-Gottesacker. *Eclogae Geologicae Helvetiae* 98, no. 1: 1–17.

Goldscheider, N., H. Hötzl, W. Käss, and W. Ufrecht. 2003. Combined tracer tests in the karst aquifer of the artesian mineral springs of Stuttgart, Germany. *Environmental Geology* 43, no. 8: 922–929.

Harvey, R.W. 1997. Microorganisms as tracers in groundwater injection and recovery experiments: A review. *FEMS Microbiology Reviews* 20, no. 3–4: 461–472.

Harvey, R.W., D.W. Metge, A.M. Shapiro, R.A. Renken, C.L. Osborn, J.N. Ryan, K.J. Cunningham, and L. Landkamer. Chemical and pathogen transport in the karst limestone of the Biscayne aquifer: 3. Use of microspheres to estimate the transport potential of *Cryptosporidium parvum* oocysts. *Water Resources Research*, submitted.

Käss, W. 1998. *Tracing Technique in Geohydrology.* Rotterdam: Balkema.

Keller, A.A., S. Sirivithayapakorn, and C.V. Chrysikopoulos. 2004. Early breakthrough of colloids and bacteriophage MS2 in a water-saturated sand column. *Water Resources Research* 40, no. 8: W08304, doi: 10.1029/2003WR002676.

Kreft, A., and A. Zuber. 1978. Physical meaning of dispersion equation and its solution for different initial and boundary conditions. *Chemical Engineering Science* 33, no. 11: 1471–1480.

Mahler, B.J., J.C. Personne, G.F. Lods, and C. Drogue. 2000. Transport of free and particulate-associated bacteria in karst. *Journal of Hydrology* 238, no 3–4: 179–193.

Mahler, B.J., P.C. Bennett, and M. Zimmerman. 1998. Lanthanide-labeled clay: A new method for tracing sediment transport in karst. *Ground Water* 36, no. 5: 835–843.

Maloszewski, P., R. Benischke, and T. Harum. 1992. Mathematical modelling of tracer experiments in the karst of Lurbach-System. *Beitr. z. Hydrogeologie* 43: 116–136.

McCarthy, J.F., and L.D. McKay. 2004. Colloid transport in the subsurface: Past, present, and future challenges. *Vadose Zone Journal* 3, no. 2: 326–337.

McDowellboyer, L.M., J.R. Hunt, and N. Sitar. 1986. Particle-transport through porous-media. *Water Resources Research* 22, no. 13: 1901–1921.

Panno, S.V. 2006. Karst aquifers: Can they be protected? *Ground Water* 44, no. 4: 494.

Pronk, M., N. Goldscheider, and J. Zopfi. 2006. Dynamics and interaction of organic carbon, turbidity and bacteria in a karst aquifer system. *Hydrogeology Journal* 14, no. 4: 473–484.

Renken, R.A., K.J. Cunningham, M.R. Zygnerski, M.A. Wacker, A.M. Shapiro, R.W. Harvey, D.W. Metge, C.L. Osborn, and J.N. Ryan. 2005. Assessing the vulnerability of a municipal well field to contamination in a karst aquifer. *Environmental & Engineering Geoscience* 11, no. 4: 319–331.

Sirivithayapakorn, S., and A. Keller. 2003. Transport of colloids in saturated porous media: A pore-scale observation of the size exclusion effect and colloid acceleration. *Water Resources Research* 39, no. 4: 1109.

Toran, L., and A.V. Palumbo. 1992. Colloid transport through fractured and unfractured laboratory sand columns. *Journal of Contaminant Hydrology* 9, no. 3: 289–303.

Toride, N., F.J. Leij, and M.T. van Genuchten. 1999. The CXTFIT code for estimating transport parameters from laboratory or field tracer experiments. Research Report No. 137. Riverside, California: US Salinity Laboratory, USDA, ARS.

Toride, N., F.J.Leij, and M.T. van Genuchten. 1993. A comprehensive set of analytical solutions for nonequilibrium solute transport with first-order decay and zero-order production. *Water Resources Research* 29, no. 7: 2167–2182.

Zhang, P., W.P. Johnson, M.J. Piana, C.C. Fuller, and D.L. Naftz. 2001. Potential artifacts in interpretation of differential breakthrough of colloids and dissolved tracers in the context of transport in a zero-valent iron permeable reactive barrier. *Ground Water* 39, no. 6: 831–840.